

**HIGH-RESOLUTION SEISMIC VELOCITY AND ATTENUATION STRUCTURE OF THE
SICHUAN-YUNNAN REGION, SOUTHWEST CHINA, USING SEISMIC CATALOG
AND WAVEFORM DATA**

Haijiang Zhang¹, Clifford H. Thurber¹, and Xiaodong Song²

University of Wisconsin¹ and University of Illinois²

Sponsored by Air Force Research Laboratory

Contract No. FA8718-05-C-0016

ABSTRACT

One of the fundamental problems facing discrimination and location of earthquakes and explosions is creating accurate structure models for the crust and mantle. The routine practice of locating seismic events based on a one-dimensional velocity model inevitably introduces bias into locations. Using a high-resolution three-dimensional seismic velocity model significantly improves seismic event location accuracy and thus helps satisfy the goal of nuclear explosion monitoring. In addition to seismic event locations, seismic wave amplitudes are also important in discriminating between earthquakes and explosions. As seismic waves travel through an anelastic and heterogeneous medium, their amplitudes will be attenuated, and knowledge of the attenuation structure is vital to correct the distortion. This two-year project is to develop high-resolution models of the velocity and attenuation structure of the Sichuan-Yunnan region (latitudes ~97-108°E and longitudes ~21-35°N) that is located in southwest China using seismic catalog and waveform data. The Sichuan-Yunnan region lies in the transition zone between the uplifted Tibetan plateau to the west and the Yangtze continental platform to the east. This region has a very complicated geological structure and is one of the most active areas of continental earthquakes in the world.

There are four main components in this project: (1) using waveform alignment methods (waveform cross-correlation and bispectrum analysis) to obtain more accurate differential arrival times, (2) using regional scale adaptive-grid double-difference tomography to obtain detailed P- and S-wave velocity models of Sichuan-Yunnan region, (3) using the adaptive-grid “triple-difference” seismic attenuation method to determine the detailed attenuation structure for both Qp and Qs for this region, and (4) assembling a ground truth database.

Our first-year effort is to determine high-resolution velocity model of the Sichuan-Yunnan region using seismic catalog and waveform data. We will first collect catalog and waveform data from the China Seismological Bureau (newly named China Earthquake Administration), Sichuan and Yunnan provincial bureaus, and the IRIS data management center. We will then apply waveform alignment methods (waveform cross-correlation and bispectrum analysis) to obtain more accurate differential arrival times. Compared to conventional threshold-based waveform cross-correlation methods, our proposed methods have the ability to improve the quality and quantity of waveform-derived differential times through a rigorous bispectrum verification process. Finally we will develop and apply regional scale adaptive-grid double-difference tomography based on tetrahedral diagrams to determine high-resolution P- and S-wave velocity models. This method deals properly with the curvature of the Earth and has the ability to automatically adapt an inversion grid according to the data distribution. As a result, the tomographic system is more stable and the regions with higher density of data are more finely characterized. Our second-year effort will be more focused on developing and applying an adaptive-grid “triple-difference” seismic attenuation method to determine the detailed attenuation structure for both Qp and Qs and assembling a ground truth database for the region of size approximately 1300 km × 1000 km.

OBJECTIVES

The routine practice of locating seismic events based on a one-dimensional velocity model inevitably introduces bias into locations. Using a high-resolution three-dimensional seismic velocity model significantly improves seismic event location accuracy and thus helps satisfy the goal of nuclear explosion monitoring. In addition to seismic event locations, seismic wave amplitudes are also important in discriminating between earthquakes and explosions. As seismic waves travel through an anelastic and heterogeneous medium, their amplitudes will be attenuated, and knowledge of the attenuation structure is vital to correct the distortion. Our research program aims to develop high-resolution models of the velocity and attenuation structure of the Sichuan-Yunnan region (latitudes $\sim 97\text{-}108^\circ\text{E}$ and longitudes $\sim 21\text{-}35^\circ\text{N}$) that is located in southwest China using seismic catalog and waveform data. This proposal falls in topic 2 (Seismic Calibration and Ground Truth Collection) in an effort to “develop models that calibrate earth velocity and attenuation structure.” The Sichuan-Yunnan region lies in the transition zone between the uplifted Tibetan plateau to the west and the Yangtze continental platform to the east. This region has a very complicated geological structure and is one of the most active areas of continental earthquakes in the world.

Our research program consists of four components: (1) using waveform alignment methods (waveform cross-correlation and bispectrum analysis) to obtain more accurate differential arrival times, (2) using regional scale adaptive-grid double-difference tomography to obtain detailed P- and S-wave velocity models of Sichuan-Yunnan region, (3) using the adaptive-grid “triple-difference” seismic attenuation method to determine the detailed attenuation structure for both Q_p and Q_s for this region, and (4) assembling a ground truth database. In this paper, we will focus on our accomplishments under components 1 and 2.

RESEARCH ACCOMPLISHED

Background

The Sichuan-Yunnan region lies in an active transition zone between the Yangtze platform to the east and the Tibetan plateau to the west and is generally believed to have had its origin in the collision between the Indian plate and the Eurasian plate about 45 Ma ago. This continental collision led to active tectonic deformation on a larger-scale and created a high level of seismicity. There are seven major active seismic zones (belts) in this region including Longmen Shan, Xianshuihe, Anninghe, Xiaojiang, Red River, Lancang-Gengma, and Tengchong-Longling (Chan et al., 2001). Most, but not all, of the earthquakes in these belts are associated with fault zones that are identified at the surface. Obtaining a high-resolution seismic velocity model for this region and precise earthquake locations will help delineate fault zones at depth more clearly and facilitate their association with surface fault traces. Several magnitude 7 earthquakes occurred in this region in the last twenty years. Recent examples are the 1995 Mengnian earthquake ($M=7.4$) and the 1996 Lijiang earthquake ($M=7.0$). The auxiliary International Monitoring Station (IMS) station KMI is located in this region and China’s nuclear test site Lop Nor is located about 1000 km to the northeast.

There have been some local to regional seismic tomography studies in this region. Chan et al. (2001) used both P and S arrival data from 4625 local and regional earthquakes recorded at 174 stations to determine a three-dimensional (3D) model of the crust. The horizontal grid spacing was 0.5 degrees between latitudes $25\text{-}34^\circ\text{N}$ and longitudes $97\text{-}105^\circ\text{E}$. They found the crustal velocity was generally a bit slow with an average value of 6.25km/s and the crustal thickness had strong lateral variations between 38km and 65km and generally increased from southeast to northwest. Yang et al. (2004) conducted a simultaneous inversion to determine the velocity models and event locations using P_g and S_g picks on 193 stations from 9988 earthquakes during the period of 1992 to 1999. Their P-wave velocity model with a horizontal grid spacing of 1° shows strong heterogeneity (contrast) across the faults. Liu et al. (2005) used a combination of 602 local and regional earthquakes and 102 teleseismic events to determine a 3D P-wave velocity model with a horizontal grid spacing of 0.5° for this region. They imaged a relatively low-velocity anomaly over a large region at depths of 20 to 50 km that may indicate a mechanically weak north-south tectonic belt between Tibet and Eastern China.

Bispectrum Method

When two earthquakes have close hypocenters and share similar source mechanisms, they will generate similar waveforms. It is possible to obtain very accurate differential times from waveform data for such nearby events and use them to improve location results (e.g., Shearer, 1997; Rubin et al., 1999; Waldhauser and Ellsworth, 2002;

Schaff et al., 2002), or combine them with absolute arrival times to invert for high-quality 3D velocity structure (Zhang and Thurber, 2003). Such studies generally use a cross correlation (CC) technique to calculate the relative time delay between the waveforms of two events recorded at the same station. For very similar traces some researchers obtain a time delay to the sub-sample level by a weighted linear fitting of the cross spectral phase after first aligning the two waveforms with the CC-determined lag (Poupinet et al., 1984). The calculated time delay has an associated CC coefficient whose value may not be very high if the underlying signals are not time-delayed similar waveforms, or if the underlying time-delayed signals are contaminated by high levels of noise. It is hard to differentiate between these two possible causes, especially when many thousands or more waveforms are being analyzed automatically. Thus researchers often choose those time delay estimates with CC coefficients above a specified threshold. For example, Schaff et al. (2002) only select those time delays with CC values larger than 0.70 and mean coherences above 0.70.

The selection of an optimum threshold value is important but difficult. If it is set too high, then only a limited number of very accurate differential time data are available to constrain the relative positions of earthquakes. If the threshold value is set too low, then many unreliable differential time estimates are used which will negatively affect the relocation results. Du et al. (2004a) deal with this problem by computing additional estimates of the time delay with the bispectrum (BS) method. The BS method, which works in the third-order spectral domain, can suppress correlated Gaussian or low-skewness noise sources (Nikias and Raghuvver, 1987; Nikias and Pan, 1988). Du et al. (2004a) adopt this method to calculate two additional time delay estimates with both the raw (unfiltered) and band-pass filtered waveforms, and use them to verify (select or reject) the one computed with the CC technique using the filtered waveforms. Thus this BS verification process can reject unreliable CC time delay estimates and also can accept additional CC time delays even if their associated CC coefficients are smaller than a nominal threshold value if they pass the BS verification procedure.

We do not claim that the BS method always obtains a better time delay estimate than the CC technique. Rather, we use the BS time delay estimates to check the reliability of those computed with the CC technique. By applying two different methods that work in different spectral domains, we can improve the reliability of the selected time delays. The two BS time delay estimates do not always agree with each other because the characteristics of noise in the raw and filtered waveforms differ. Therefore checking the values of the CC time delay against both of them provides additional quality control.

Figure 1 shows four seismic waveforms (sampling rate=0.025s) from the Incorporated Research Institutions for Seismology (IRIS) Data Management Center recorded on the auxiliary IMS station KMI. These events are far apart from each other, up to several tens of kilometers away. But using the BS analysis, we are still able to extract the differential arrival times between event 19862792328 (top) and the other three events (19892630026, 19953311008, and 19953331916). The waveform correlation coefficients between the top waveform and the bottom three waveforms are 0.83, 0.80 and 0.71, respectively. The time window we choose here is 30 samples before and 97 samples after the preliminary P arrival picks. The results went through the BS verification process successfully. This example shows that we can obtain a substantial amount of waveform alignment data when we have access to local network waveforms.

Double-difference tomography

We have recently developed a double-difference (DD) seismic tomography method that makes use of both absolute and more accurate relative arrival times (Zhang and Thurber, 2003). DD tomography is a generalization of DD location (Waldhauser and Ellsworth, 2000); it simultaneously solves for the three-dimensional (3D) velocity structure and seismic event locations. DD tomography uses an evolving weighting scheme for the absolute and differential arrival times in order to determine the velocity structure from larger scale to smaller scale. This method yields more accurate event locations and velocity structure near the source region than standard tomography, which uses only absolute arrival times. It has the unique ability to sharpen the velocity image near the source region because of the combination of the higher accuracy of the differential time data and the concentration of the corresponding model derivatives in the source region. The latter results from the cancellation of model derivative terms where the ray paths overlap away from the source region.

To date, we have applied DD tomography to several synthetic datasets, to the Hayward fault dataset of Waldhauser and Ellsworth (2002) (Zhang and Thurber, 2003), to data from Parkfield, California (Thurber et al., 2004), and to data from northern Honshu, Japan (Zhang et al., 2004). The Hayward and Parkfield studies used a flat-earth version

of the DD tomography code (*tomoDD*) with pseudo-bending ray tracing (Um and Thurber, 1987), whereas the Japan study used a “sphere-in-a-box” version (*tomoFDD*) with finite-difference travel time calculations (Podvin and Lecomte, 1991). We have carried out synthetic tests with both versions. In all cases, we can see a “sharpening” of the velocity structure and/or a revelation of previously undetected features. Both the algorithms *tomoDD* and *tomoFDD* can use a nonuniform but regular inversion grid.

In the “sphere-in-a-box” version of DD tomography, the curvature of the Earth is explicitly taken into account. We note that the earth flattening transformation approach is only valid for 1D velocity models and not for 3D velocity models so that approach is not a viable one. Following Flanagan et al. (2000), we solve this problem by parameterizing a spherical surface inside a Cartesian volume of grid nodes. Figure 2a shows the case of putting the Earth into a cube so the curvature of the Earth can be taken into account. This scheme can be used for global seismic tomography. For regional seismic tomography, we are only interested in a part of the Earth and we can construct a rectangular box covering the portion of interest (Figure 2b and c). The coordinate center is placed at the surface of the Earth, positive X and Y-axes point to the direction of north and west, and the positive Z-axis points downward. The grid nodes above the Earth’s surface (air nodes) are given the velocity for P waves traveling in air (Figure 2c). As a result, all the rays travel inside the Earth. Here we should emphasize that this version is still based on Cartesian coordinate system and not on a true spherical system.

Finite-difference ray tracing algorithms require a uniformly spaced velocity (or slowness) grid (Podvin and Lecomte, 1991). We interpolate the velocity values on the regular uniform grid nodes from non-uniform inversion grid nodes through trilinear interpolation. First we treat each station as a source and calculate travel times to all velocity nodes in the volume. The travel time from a station to each earthquake is interpolated from its 8 neighboring nodes through trilinear interpolation. The ray path from the earthquake to the station is found iteratively with increments opposite to the travel time gradient. The corresponding partial derivatives of travel times with respect to the slowness models are calculated by dividing the ray paths into small segments (Thurber, 1983).

Both the algorithms *tomoDD* and *tomoFDD* are based on a regular inversion grid. We recently developed an adaptive-mesh DD tomography method based on tetrahedral and Voronoi diagrams to automatically match the inversion mesh to the data distribution (Zhang and Thurber, 2005). Both tetrahedral and Voronoi diagrams have been shown to be powerful tools to represent spatial relationships in three dimensions and they allow a more flexible representation of the model. For example, model volumes of widely varying sizes with complex distributions are easily implemented, and it is more convenient to build parameterizations containing particular interfaces, on which the nodes can be distributed.

Linear and natural-neighbor interpolation methods can be derived for tetrahedral and Voronoi diagrams, respectively. Linear interpolation uses 4 tetrahedron nodes to interpolate the velocity/slowness values at any point and it has the advantage of calculating the interpolating basis functions easily and quickly. However, the linear interpolation function is not continuously differentiable, which is a desired property for some applications. In comparison, the natural-neighbor interpolation method interpolates the value at any point from its n natural neighbors. The natural-neighbor interpolation function guarantees continuity in first and second derivatives except at the nodes (Sambridge et al., 1995). Our algorithm allows the use of either approach.

We start the inversion from a regular inversion grid, equivalent to that of *tomoDD*. We randomly perturb the starting regular inversion grid by a very small amount (so that the nodes are not located on the same plane) in order to construct the tetrahedral or Voronoi diagram around these nodes using the Qhull algorithm (<http://www.thesa.com/software/qhull/>). We also construct a regular computational grid that remains fixed during the inversion, which can be the same as the starting regular inversion grid or finer. We trace rays between events and stations based on the current regular velocity grid. The rays between all the event and station pairs are saved for later use in defining the adaptive mesh. Using these rays, we find the partial derivatives of the travel times with respect to the model slowness parameters on the current inversion mesh. In the process, we calculate the derivative weight sum (DWS) values on the inversion mesh nodes (Thurber and Eberhart-Phillips, 1999). Threshold DWS values are set to add or remove nodes.

After this refining process, we obtain a new irregular inversion mesh, which cannot be guaranteed to be optimally data-adaptive. We construct a new tetrahedral or Voronoi diagram around the new irregular inversion mesh and recalculate the DWS values on all the nodes using the previously saved ray information. The threshold checking is repeated to determine the inversion mesh to be used for the current iteration of simultaneous inversion. Finally, a

new tetrahedral or Voronoi diagram is constructed and the partial derivatives of the travel times with respect to the new set of inversion mesh nodes are calculated for the construction of the seismic tomography equations. After each simultaneous inversion, the velocity values on the irregular inversion mesh nodes and the regular computational grid nodes are updated. For subsequent simultaneous inversions, the inversion mesh is again updated following the same procedure to better match with the ray distribution, which will change as the velocity model changes and hypocenters move.

Once the inversion mesh is set up and the partial derivatives of travel times with respect to the event locations and slowness model parameters are determined, we can construct the linear system of equations to solve for the event locations and slowness perturbations at the irregular mesh nodes in a similar way to the case of the regular inversion grid. Currently, we have finished the implementation of adaptive-grid scheme on the flat-model version of DD tomography (Zhang and Thurber, 2005). We are now in the process of implementing the adaptive-mesh scheme on the “sphere-in-a-box” version of DD tomography and will apply it to the Sichuan-Yunnan region, both as a whole and in the higher-resolution subregions we identify.

Preliminary result

At present, we have collected ~14800 catalog P and S picks from ~2080 events recorded on 63 stations covering a subregion of latitude 21° to 30° and longitude 96° to 105° (Figure 3). One part of the data is from the provincial bulletins compiled by the Yunnan and Sichuan Seismological Bureaus during the period of 1993 to 1997. Since this dataset was originally used by Liang et al. (2004) for Pn tomography in China, the distances between events and stations are generally greater than 1 degree. As a result, we only have ~3400 absolute P arrivals from ~800 events and ~60 stations. The other part of the data consists of P and S picks from the Annual Bulletin of Chinese Earthquakes (ABCE) during the period of 1990 to 2001, extracted from the dataset for China compiled by Sun (2005). We constructed ~73500 catalog differential times from event pairs within 40 km. In total, there are ~88000 catalog absolute and differential times for inversion, among which the number of P picks is twice that of S picks. The inversion grid spacing in the horizontal direction is 50 km and 5 km in the vertical direction (Figure 3). We start the inversion from a 1D velocity model and alternate between the simultaneous determination of velocity model and event locations and the determination of locations only.

The weighted root mean square (RMS) arrival time residual decreases from 37.348 s at the beginning of the inversion to 864 ms after the final iteration. Figures 4 and 5 show horizontal sections of P- and S-wave velocity models at a depth of 15 km and two cross-sections of P- and S-wave velocity models through latitudes of 23.6° and 26° , respectively. The inversion has revealed some interesting features of the region. The high plateau of the Southeastern margin of the Tibetan Plateau is remarkably well delineated by high crustal velocities (from $\sim 22^{\circ}$ N to $\sim 29^{\circ}$ N in latitude and from $\sim 99^{\circ}$ E to $\sim 103^{\circ}$ E in longitude) (Figure 4). The stable Yangtze Craton to the east has relatively low crustal velocity compared with the high plateau (Figures 4 and 5). To the west of longitude $\sim 99^{\circ}$, the western Yunnan and Myanmar regions also have relatively low crustal velocity, which correlates with the presence of a number of active volcanoes in the region (Figures 4 and 5) (Liang et al., 2004). Both horizontal slices and cross sections show strong lateral velocity heterogeneities, consistent with the nature of active fault zones in this region. Strong velocity contrasts are evident across major faults, such as Xiaojiang Fault and Red River Fault (Figure 5). The relocated earthquakes show relatively well-defined vertical linear features, corresponding to major faults at the surface (Figure 5). Recent application of DD location in this region (Yang et al., 2003) also showed that the relocated events are more concentrated near the fault zones using just the catalog differential data. We are confident that with much more local catalog data and new digital waveform data, we will be able to characterize the velocity structure at much higher resolution and obtain greatly improved earthquake locations.

CONCLUSIONS AND RECOMMENDATIONS

We have applied the “sphere-in-a-box” version of DD tomography code to a subregion of latitude 21° to 30° and longitude of 96° to 105° of the planned Sichuan-Yunnan study region using catalog picks. Both P- and S-wave velocity models show strong velocity heterogeneities, consistent with the nature of active transition zone between the Yangtze platform to the east and the Tibetan plateau to the west. Strong velocity contrasts are evident across some major fault zones and the relocated earthquakes show relatively well-defined vertical linear feature.

We are in the process of developing the adaptive-mesh “sphere-in-a-box” version of the DD tomography code and we are nearly finished with this task. Dr. Song is traveling in China in July to obtain more catalog picks and

27th Seismic Research Review: Ground-Based Nuclear Explosion Monitoring Technologies

waveform data. Once we have more data available, we can further improve the resolution of the velocity model and the accuracy of event locations in the Sichuan-Yunnan region.

ACKNOWLEDGEMENTS

We thank Megan Flanagan for allowing us to use her code in our “sphere-in-a-box” version of the DD tomography code. We are grateful to Youshun Sun for providing us his compiled picks for the Sichuan-Yunnan region.

REFERENCES

- Chan, W. W., C. Y. Wang, and W. D. Mooney (2001), 3-D crustal structure in southwestern China, in *Proceedings of the 23rd Seismic Research Review: Worldwide Monitoring of Nuclear Explosions*, LA-UR-01-4454, Vol. I, pp. 12–20.
- Du, W.X., C. H. Thurber, and D. Eberhart-Phillips (2004a), Earthquake relocation using cross-correlation time delay estimates verified with the bispectrum method, *Bull. Seismol. Soc. Am.* 94: 856–866.
- Du, W., C. H. Thurber, M. Reyners, D. Eberhart-Phillips, and H. Zhang (2004b), New constraints on seismicity in the Wellington region of New Zealand from relocated earthquake hypocentres, *Geophys. J. Int.* 158: 1088–1102.
- Flanagan, M. P., S.C. Myers, C. A. Schultz, M. E. Pasyanos, and J. Bhattacharyya (2000), Three-dimensional a priori model constraints and uncertainties for improving seismic location, in *Proceedings of the 22nd Annual DoD/DOE Seismic Research Symposium: Planning for Verification of and Compliance with the Comprehensive Nuclear-Test-Ban Treaty (CTBT)*, Vol. 2, pp. 129-136.
- Kim, W.-Y., D. P. Schaff, J. Zhang, F. Waldhauser, and P. G. Richards (2004), Evaluation of cross-correlation methods on a massive scale for accurate relocation of seismic events, in *Proceedings of the 26th Seismic Research Review: Trends in Nuclear Explosion Monitoring*, LA-UR-04-5801, Vol. 1, pp. 277–286.
- Liang, C. T., X. D. Song, J. L. Huang (2004), Tomographic inversion of Pn travel-times in China, *J. Geophys. Res.* 109, B11304, doi:10.1029/2003JB002789.
- Liu, Y., X. Xhang, J. He, F. Liu, and H. Sun (2005), Three-dimensional velocity images of the crust and upper mantle beneath the north-south zone in China, *Bull. Seismol. Soc. Am.* 95: 916–925.
- Nikias, C. L., and R. Pan (1988), Time delay estimation in unknown Gaussian spatially correlated noise, *IEEE Trans. Acoust. Speech Signal Process* 36: 1706–1714.
- Nikias, C. L., and M. R. Raghuveer (1987), Bispectrum estimation: A digital signal processing framework, *Proc. IEEE* 75: 869–891.
- Podvin, P., and I. Lecomte (1991), Finite difference computation of travel times in very contrasted velocity models: a massively parallel approach and its associated tools, *Geophys. J. Int.* 105: 271–284.
- Poupinet, G., W. L. Ellsworth, and J. Frechet (1984), Monitoring velocity variations in the crust using earthquake doublets: An application to the Calaveras Fault, California, *J. Geophys. Res.* 89: 5719–5713.
- Rubin, A. M., D. Gillard, and J. L. Got (1999), Streaks of microearthquakes along creeping faults, *Nature* 400: 635–641.
- Sambridge, M., Braun, J., and McQueen, H. (1995), Geophysical parametrization and interpolation of irregular data using natural neighbours, *Geophys. J. Int.* 122: 837–857.
- Schaff, D. P., and P. G. Richards (2004), Repeating seismic events in China, *Science* 303: 1176–1178.
- Schaff, D. P., G. H. R. Bokelmann, G. C. Beroza, F. Waldhauser, and W. L. Ellsworth (2002), High-resolution image of Calaveras Fault seismicity, *J. Geophys. Res.* 107, 2186, doi:10.1029/2001JB000633.

27th Seismic Research Review: Ground-Based Nuclear Explosion Monitoring Technologies

- Shearer, P. M. (1997), Improving local earthquake locations using the L1 norm and waveform cross correlation: application to the Whittier Narrows, California, aftershock sequence, *J. Geophys. Res.* 102: 8269–8283.
- Sun, Y. (2005), P- and S-wave tomography of the crust and uppermost mantle in China and surrounding areas, PhD dissertation, Massachusetts Institute of Technology, 314 pp.
- Thurber, C. H. (1983), Earthquake locations and three-dimensional crustal structure in the Coyote Lake area, central California, *J. Geophys. Res.* 88: 8226–8236.
- Thurber, C., and D. Eberhart-Phillips (1999), Local earthquake tomography with flexible gridding, *Comp. & Geosci.* 25: 809–818.
- Thurber, C., S. Roecker, H. Zhang, S. Baher, and W. Ellsworth (2004), Fine-scale structure of the San Andreas fault and location of the SAFOD target earthquakes, *Geophys. Res. Lett.* 31, doi:10.1029/2003GL019398.
- Um, J., and C. H. Thurber (1987), A fast algorithm for two-point seismic ray tracing, *Bull. Seism. Soc. Am.* 77: 972–986.
- Waldhauser, F. and W. L. Ellsworth (2000), A double-difference earthquake location algorithm: Method and application to the northern Hayward fault, CA, *Bull. Seismol. Soc. Am.* 90: 1353–1368.
- Waldhauser, F., and W. L. Ellsworth (2002), Fault structure and mechanics of the Hayward Fault, California, from double-difference earthquake locations, *J. Geophys. Res.* 107: ESE 3-1-3-12.
- Yang, Z., Y. Chen, Y. Zheng, and X. Yu (2003), Accurate relocation of earthquakes in central-western China using the double-difference earthquake location algorithm, Science in China (Series D), *Sci. China (D)* 46: 129–134.
- Yang, Z.-X., X.-W. Yu, Y.-J. Zheng, Y.-T. Chen, X.-X. Ni, and W. Chan (2004), Earthquake relocation and 3-dimensional crustal structure of P-wave velocity in central-western China, *Acta Seismologica Sinica* 17: 20-30.
- Zhang, H., and C.H. Thurber (2003), Double-difference tomography: method and application to the Hayward fault, California, *Bull. Seismol. Soc. Am.* 93: 1875–1889.
- Zhang, H., and C. Thurber (2005), Adaptive mesh seismic tomography based on tetrahedral and Voronoi diagrams: Application to Parkfield, California, *J. Geophys. Res.* 110, B04303, doi:10.1029/2004JB003186.
- Zhang, H., C. Thurber, D. Shelly, S. Ide, G. Beroza, and A. Hasegawa (2004), High-resolution subducting slab structure beneath Northern Honshu, Japan, revealed by double-difference tomography, *Geology* 32: 361–364.

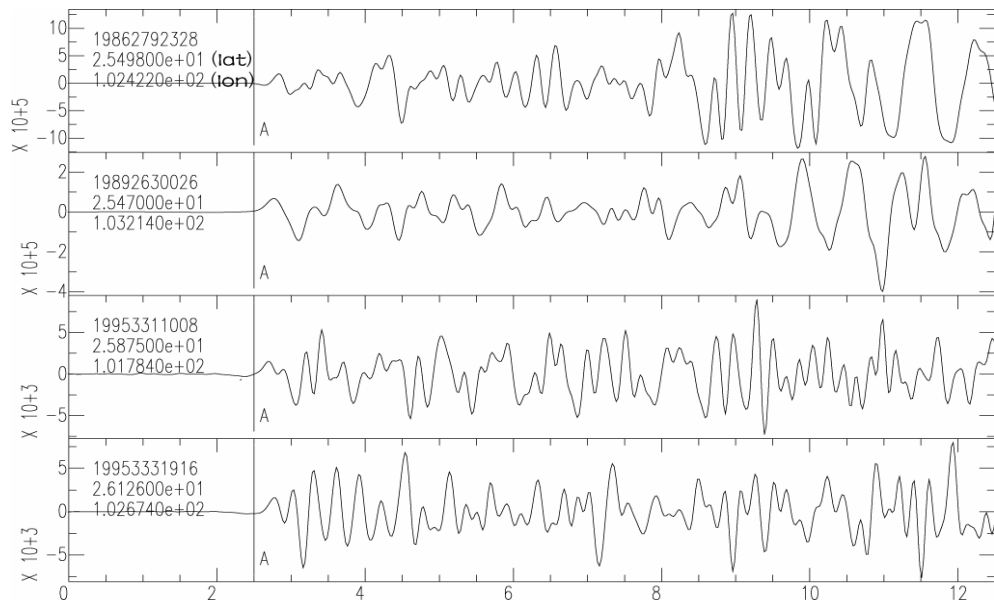


Figure 1. Seismic waveforms recorded on station KMI.

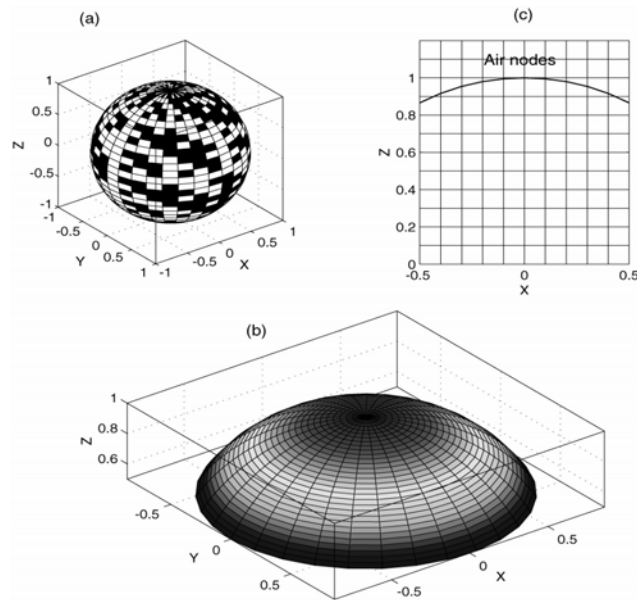


Figure 2. Grid setup for regional scale double-difference tomography. (a) The whole earth is inserted into a cubic box. (b) A rectangular box covers the region of interest. (c) The representation of (b) in the X-Z plane. The surface of the Earth is shown as a thick line. The regular grid is used for finite-difference ray tracing algorithm.

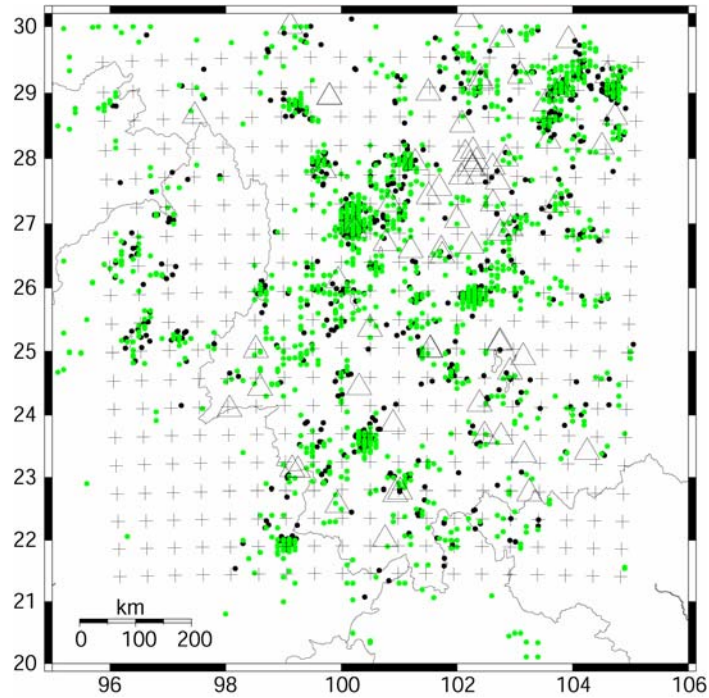


Figure 3. Event and station distribution map. Events and stations are indicated by dots and triangles, respectively. Black dots indicate events compiled by the Yunnan and Sichuan Seismological Bureaus, whereas green ones are from the Annual Bulletin of Chinese Earthquakes. Crosses are inversion grid nodes in the horizontal plane.

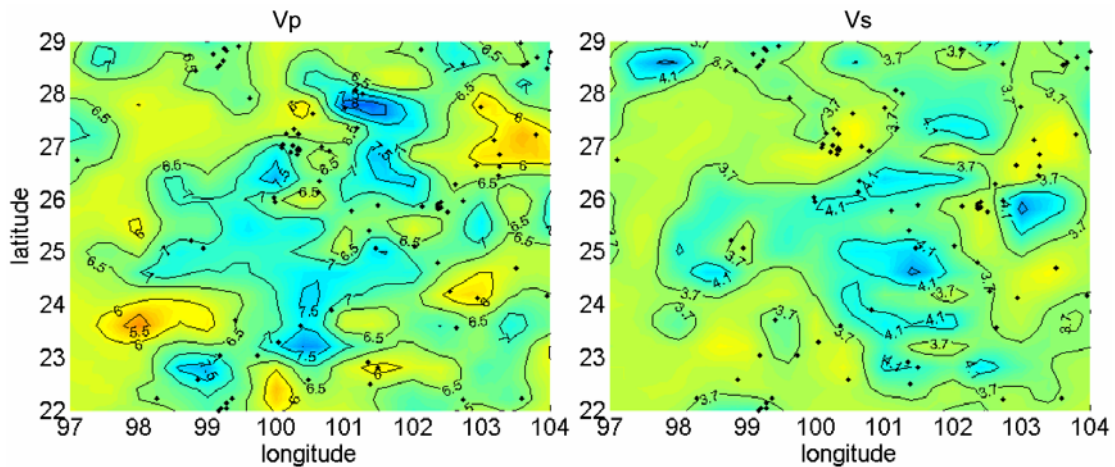


Figure 4. Horizontal sections of the P- and S-wave velocity models at a depth of 15 km. Black dots are seismic events within 2.5 km of this section.

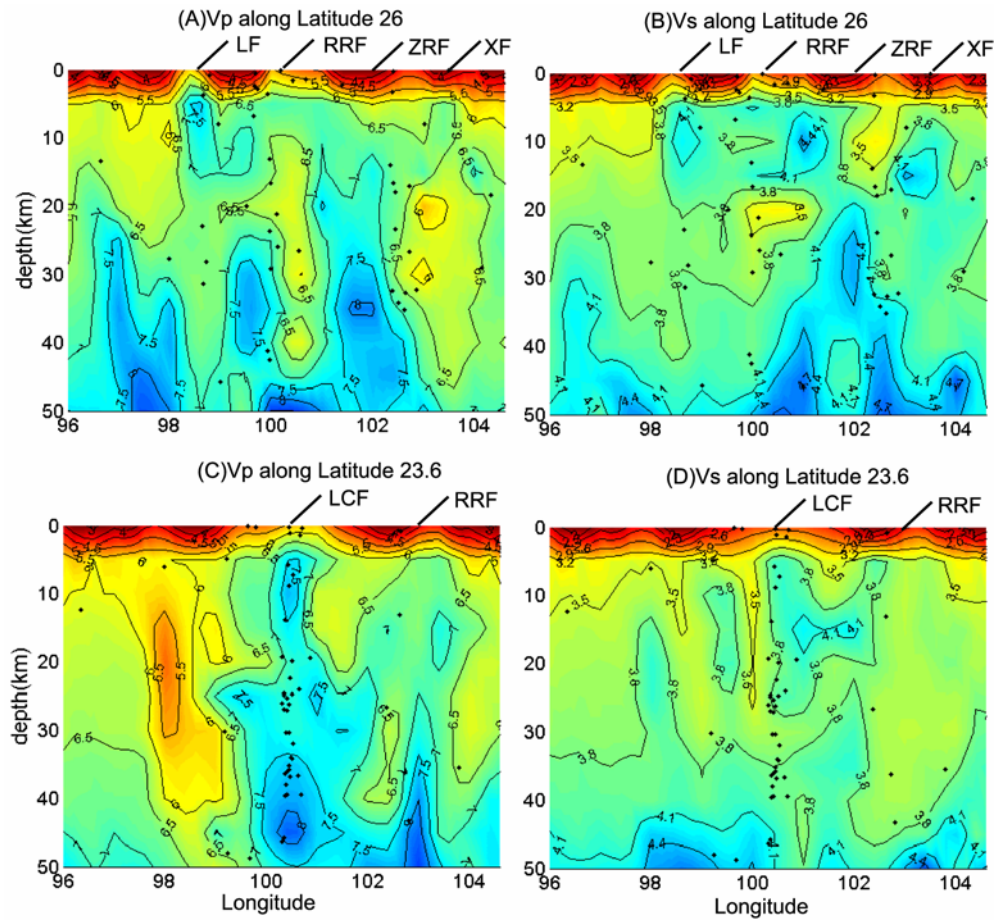


Figure 5. Cross-sections of P- and S-wave velocity models along latitudes 26° and 23.6° . LF - Longling Fault, RRF - Red River Fault, XF - Xiaojiang Fault, LCF - Lancang River Fault, ZRF - Zemu River Fault.